JOURNAL OF MATERIALS SCIENCE 14 (1979) 1681–1693

Partial replacement of cement by fly ash in autoclaved products – theory and practice

J. J. BEAUDOIN, R. F. FELDMAN
Materials Research, Division of Building Research, National Research Council of Canada, Ottawa K1A OR6, Canada

Nine different fly ashes have been used in a study of autoclaved (216° C) cement–fly ash mixtures containing 50% fly ash (by weight). Paste samples for each fly ash were prepared at water–solid ratios of 0.22 to 0.45 and mechanical property–porosity relations were determined. The autoclaved products were characterized by several techniques. Linear correlations with a composition term, $C/(S + A) - kF$, were obtained for logarithms of zero-porosity modulus of elasticity and microhardness values. A linear correlation for modulus of elasticity of the porous solid and the composition term, $2 - C/(S + A) - kF$, was also obtained for each water–solid ratio. Correlations for microhardness of the porous solid with a composition term, $2 - C/(S + A)$ are reported, a different curve for each water–solid ratio. Impregnation of the porous products resulted in increased values for modulus of elasticity and microhardness and provided an alternate means of estimating zero-porosity values of these properties.

1. Introduction

Energy conservation in the building industry is a world-wide concern. As one response to the challenge, engineers and scientists are exploring ways of producing building materials with a minimum of energy input, and interest in the use of waste material such as fly ash as a partial replacement for Portland cement in concrete products, although not new, is growing [1–3].

There is advantage in adding fly ash to concrete products cured at normal atmospheric conditions or in the autoclave at high temperatures and pressures. In the autoclave, high-pressure steam curing without the addition of finely divided silica produces generally weak, porous bodies consisting of dense, crystalline hydrated material, usually αC_2S hydrate [4]. An optimum amount of finely divided silica promotes the formation of tobermorite and poorly crystallized CSH(I), generally giving maximum strength. Using fly ash as a source of silica in autoclaved materials may be expected to result in the formation of hydrated products similar to those formed by adding pure silica [5]. As fly ash is more complex than silica, however, and contains CaO, Al_2O_3, Fe_2O_3 and other impurities, its composition is dependent on the source and operational conditions at each power plant and it is of practical importance to evaluate the effect of composition on the mechanical properties of building products.

In order to predict the properties of autoclaved cement–fly ash mixtures, an understanding is essential of the hydration reactions and of the products formed and their mechanical properties. This can be achieved by studying the modulus of elasticity (or microhardness)–porosity relations and correlating zero-porosity values of modulus of elasticity and microhardness with the chemical composition of several fly ash–cement mixtures.

Previous studies of autoclaved Portland cement–silica mixtures have shown that where weak porous matrices are formed (because they consist mainly of dense crystalline products), high strength can be obtained by impregnating these bodies with sulphur [6]. It was the object of this study to gain an understanding of the reactions that occur when autoclaving different fly ash–cement mixtures and to develop equations by

0022–2461/79/071681–13 $3.30/0

TABLE I Chemical analysis of fly ash and portland cement

Fly ash	SiO_2	Al_2O_3	MgO	Fe_2O_3	CaO	N_2O	K_2O	Loss on ign.	Other	C/(S + A)* (mole ratio)
1	51.54	25.08	0.16	10.58	4.81	0.49	2.39	4.08	0.87	0.769
2	39.78	22.30	0.27	9.12	16.58	1.61	1.16	1.25	7.93	1.057
3	40.86	21.62	0.28	6.26	22.44	0.53	0.79	0.65	6.57	1.123
4	34.22	19.58	1.16	16.99	7.00	0.51	1.67	18.15	0.72	1.027
5	45.86	25.62	1.29	18.09	7.35	0.55	1.95	0.00	0.00	0.852
6	44.66	22.74	3.31	4.20	14.27	1.68	0.98	0.37	7.79	0.962
7	55.27	22.59	0.94	3.85	12.14	0.34	1.04	0.52	3.31	0.830
8	40.21	19.42	0.38	13.05	3.50	0.61	1.37	13.09	8.37	0.901
9	45.35	20.85	0.42	17.84	3.87	0.59	1.47	1.04	8.57	0.839
PC	20.66	6.22	1.28	2.16	64.45	0.08	1.30	–	3.85	–

* Includes both fly ash and cement constituents

which the mechanical properties of any autoclaved fly ash–cement mixture may be predicted. The potential use of such products impregnated with sulphur was an additional area of investigation.

2. Experimental details

2.1. Materials

(1) Normal type I Portland cement was used for all mixes; the chemical analysis is presented in Table I.

(2) Fly ash. Fly ash samples were obtained from nine different locations; chemical analysis is presented in Table I. The calculated C/(S + A)* mole ratio for each cement–fly ash mixture (50/50 by weight) is also included in Table I. All C/(S + A) mole ratios referred to in this work are for the total cement plus fly ash mixture.

(3) Sulphur. Reagent-grade sulphur containing 3 ppm H_2S.

2.2. Methods

2.2.1. Hydration

Samples were prepared for autoclaving at water–solid ratios of 0.22, 0.26, 0.30, 0.35, 0.40 and 0.45. The solids for all mixes contained 50% Portland cement and 50% fly ash. At each water–solid ratio, nine sets of samples were prepared, each utilizing a different fly ash. Mixes were cast in cube moulds, three cubes for each preparation, and moist-cured for 24 h. After demoulding, samples were autoclaved at 216° C, 2.04 MPa pressure, for 3 h. A 32 mm core was obtained from the cube samples for each preparation. Ten discs, 1.27 mm thick, were sliced from each core for measurement of modulus of elasticity and microhardness.

Samples containing fly ash no. 3 cracked during autoclaving. It was therefore necessary to autoclave fly ash 3 by itself, followed by drying and sieving through 100-mesh screen prior to mixing with cement. The test series using fly ash 3 was prepared in this manner.

2.2.2. Chemical analysis

Chemical analysis was performed by Atomic Absorption Spectrophotometry using a Perkin-Elmer 403 AAS.

2.2.3. Helium diffusion measurements

A set of samples having approximately the same porosity (32.5%) was chosen for each fly ash for helium diffusion measurements. The apparatus and procedure for helium diffusion measurements have been described in detail in previous papers [7, 8]. Small spaces or "pores" into which helium does not instantaneously flow are, in the first instance, regarded as part of the solid. Subsequent intake of helium with time was recorded. Samples were conditioned at 11% r.h. prior to diffusion measurements.

2.2.4. Sulphur impregnation

Samples used for helium diffusion studies were also used for sulphur impregnation work. Three discs from each set of samples were impregnated using the technique described previously [6]. Modulus of elasticity and microhardness measurements were also made on these samples.

2.2.5. Differential scanning calorimeter (DSC)

Differential thermograms of the samples were obtained by a differential scanning calorimeter

* In cement nomenclature C = CaO, A = Al_2O_3, F = Fe_2O_3, S = SiO_2, and H = H_2O.

(DSC) supplied as a module to the DuPont 990 thermal analysis system. The heating rate was 20° C min^{-1}. Differential temperature was registered at a sensitivity of 0.02 mV $in.^{-1}$. Thermograms were obtained in air and in each experiment 20 mg sample was subjected to analysis.

2.2.6. Surface area

Surface area was obtained with N_2 as the absorbate by a Numinco-Orr surface-area pore volume analyser. Each sample was dried at 110° C for 3 h prior to analysis.

2.2.7. X-ray diffraction (XRD)

X-ray powder photographs were obtained with a Philips camera using a Cu$K\alpha$ source. Relative intensities of the lines were obtained by densitometer traces of the powder photographs.

2.2.8. Scanning electron miscroscope (SEM)

Microstructural examination was conducted on fractured pieces of the specimens by means of a Cambridge Stereoscan Mark 2A.

2.2.9. Helium comparison pycnometry

Porosity was determined using a helium comparison pycnometer. The application of this technique to the hydrated Portland cement system is described elsewhere [9]. Solid volume is measured, enabling determination of porosity using the apparent volume calculated from sample geometry. The problem of rehydration encountered when water is used as the displacement medium is avoided. Using 11% r.h. as datum avoids excessive decomposition of the hydrates.

2.2.10. Modulus of elasticity and microhardness

Modulus of elasticity was measured on 3.2 cm diameter discs 1.3 mm thick, at least three discs for each set of samples. The procedure involves measuring the deflection of a specimen loaded at its centre and supported at three points on the circumference of a circle 2.5 cm diameter [10]. A Leitz microhardness testing machine with a Vickers indenter was used for microhardness measurements, which were made on the discs used for modulus of elasticity measurements and were carried out at 11% r.h. Five hardness measurements were made on each disc and three discs were tested for each set of samples.

3. Results

The results will be presented in three sections. The first is concerned with basic physico–mechanical properties of the autoclaved cement–fly ash mixtures and the correlation between these properties and composition of the fly ash and cement. In the second section, the mechanical properties are presented in terms of water–solid ratio as well as a term dependent on composition of the cement–fly ash mixture. In the third section, data are presented illustrating the potential of autoclaved cement–fly ash mixtures for use in impregnated systems.

3.1. Physico–mechanical properties

3.1.1. Mechanical property–porosity relations

The data for all preparations (nine fly ashes) obey the general relation

$$H,E = (H_0,E_0) \exp(-b_{H,E} \cdot p)$$

where H,E refer to microhardness and modulus of elasticity and p is porosity. The results of linear regression analysis are recorded in Table II. Regression lines of log microhardness and modulus of elasticity versus porosity are given in Figs. 1 and

TABLE II Regression analysis of microhardness and modulus of elasticity versus porosity relations

Fly ash	$H = H_0 \exp(-b_H \cdot p)$			$E = E_0 \exp(-b_E \cdot p)$		
	H_0 (MPa × 10^{-1})	b_H	r (%)	E_0 (MPa × 10^{-3})	b_E	r (%)
1	60.68	0.028	83.5	26.82	0.015	75.8
2	151.70	0.069	98.3	36.82	0.031	94.5
3	342.80	0.061	91.0	53.00	0.035	90.2
4	100.00	0.051	95.9	25.30	0.026	86.6
5	83.18	0.035	89.3	31.77	0.024	96.6
6	206.55	0.065	97.1	50.15	0.035	97.0
7	66.53	0.034	90.7	43.85	0.033	95.5
8	100.00	0.062	92.7	35.16	0.028	73.3
9	84.34	0.062	90.6	44.67	0.054	91.9

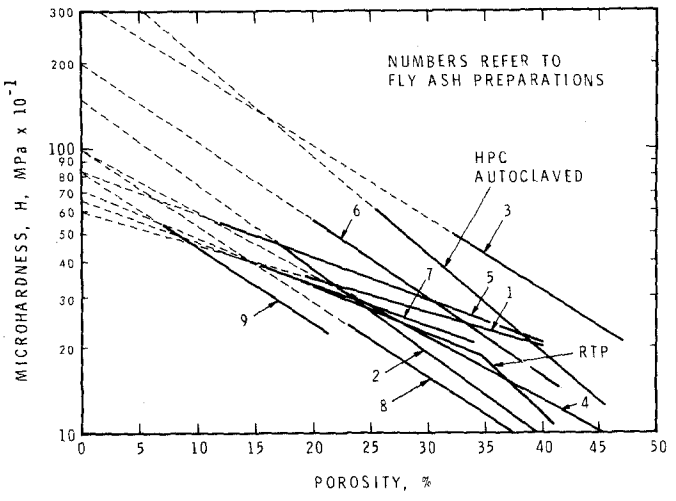

Figure 1 Microhardness versus porosity curves for autoclaved cement–fly ash mixtures.

2; there is a different linear relation for each preparation.

3.1.2. Physical properties of hydration products

Measurements were taken of solid density, surface area, and total He intake at 11% r.h. (Table III). Tabulated densities ($\bar{\rho}$) are average values of six sets of samples (w/s = 0.22 to 0.45) for each fly ash preparation. Densities range from 2.23 for fly ash 9 to 2.76 for fly ash 3. Samples having w/s = 0.22 generally have lower densities than those having higher w/s ratios; these values are included in the average calculation and do not significantly affect the result. Surface areas range from 17.0 to 25.5 $m^2 g^{-1}$.

A number of relations were determined for mechanical properties of the hydrated solid, composition and physical properties. These are listed. The logarithm of the composition term C/(S + A) $-kF$ is plotted against solid density in Fig. 3 in which a linear dependence can be seen. The composition terms are expressed in mol%, and k is a constant = 1.60. The value of k chosen was that giving the best correlation coefficient.

TABLE III Some physical properties of autoclaved cement–fly ash mixtures

Fly ash	Solid density $\bar{\rho}$ (g cm^{-3})	Surface area ($m^2 g^{-1}$)	Total He intake ($cm^3 g^{-1}$ × 10^2)
1	2.29	23.5	4.53
2	2.46	21.3	2.33
3	2.76	21.1	1.84
4	2.37	18.1	2.47
5	2.34	25.4	3.41
6	2.42	23.0	4.30
7	2.24	21.3	6.58
8	2.40	17.0	3.32
9	2.23	25.5	5.11
RTP w/c = 0.40	2.20	≃ 50.0	4.20

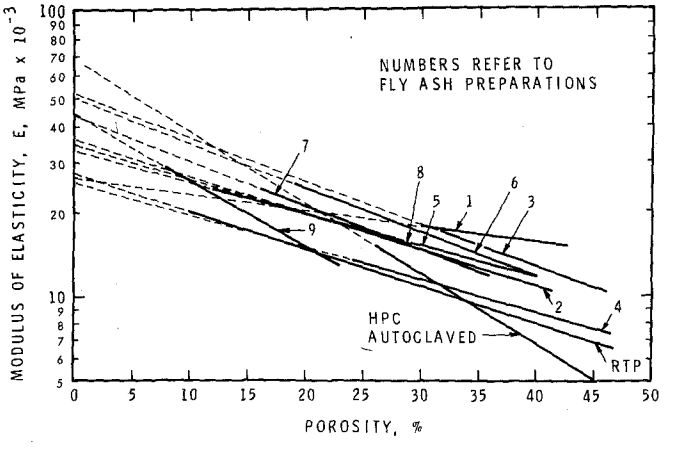

Figure 2 Modulus of elasticity versus porosity curves for autoclaved cement–fly ash mixtures.

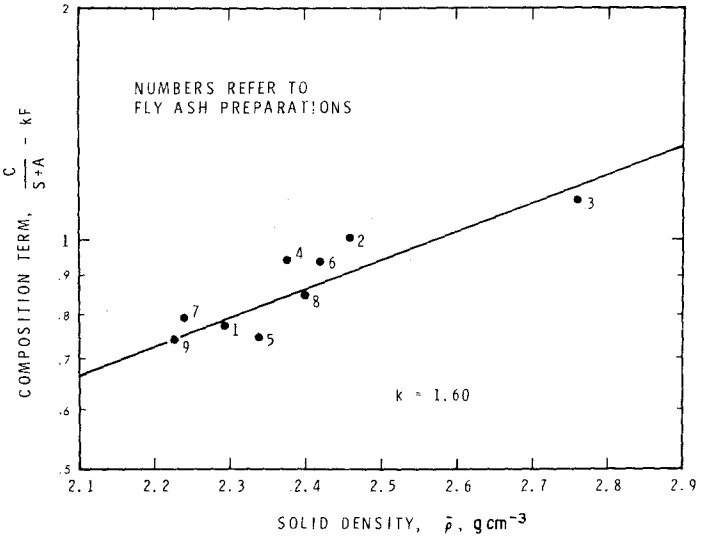

Figure 3 Composition term, C/(S + A) − kF, versus solid density of autoclaved cement–fly ash mixtures.

The total helium intake increases with decrease in solid density, as can be seen in Fig. 4; and there is a linear dependence between the logarithm of zero porosity microhardness, H_0, and solid density (Fig. 5). The logarithm of zero porosity microhardness also depends linearly on C/(S + A) − kF (k = 1.60) (Fig. 6).

The logarithm of zero-porosity modulus of elasticity, E_0, depends linearly on C/(S + A) − kF and the best correlation is obtained with k = 8.00 (Fig. 7). The plot point representing fly ash no. 9 did not appear to conform to the data and was not included in the regression analysis.

Equations obtained by regression analysis for the lines plotted in Figs. 3 to 7 are given in Table IV.

3.1.3. Characterization of hydrated products

3.1.3.1. Differential thermal analysis. DSC traces are presented in Fig. 8, all exhibiting a small quartz peak at 550° C. A small endotherm at 470° C resulting from decomposition of $Ca(OH)_2$ is present for preparations 1, 3, 6 and 7. An endotherm at approximately 100° C, preparations 1, 2, 4, 8 and 9, may be due to decomposition of C–S–H gel.

3.1.3.2. SEM. Scanning electron micrographs for the nine autoclaved cement–fly ash mixtures are presented in Fig. 9. They are generally representative of the microstructure throughout each sample. Preparations 3, 4, 7 and 8 contain fibrous

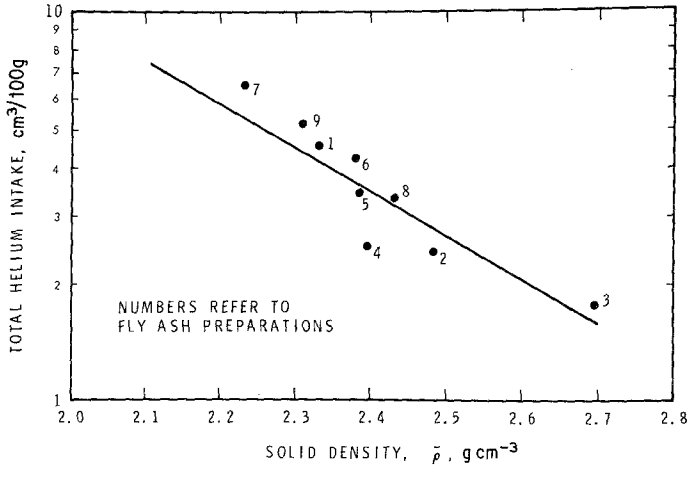

Figure 4 Total helium intake versus solid density of autoclaved cement–fly ash mixtures.

TABLE IV Regression analysis for curves plotted in Figs. 3 to 7

	Equation	Correlation coefficient, r (%)	Figure
1	$C/(S + A) - kF = 0.134 \exp(+ 0.775\bar{\rho})$ $k = 1.60$	83.0	3
2	$He = 1738 \exp(-2.59\bar{\rho})$ $(2.23 < \bar{\rho} < 2.70)$	89.2	4
3	$H_0 = 0.052 \exp(3.22\bar{\rho})$	90.4	5
4	$H_0 = 3.95 \exp\{3.89 [C/(S \times A) - kF]\}$ $k = 1.60$	89.4	6
5	$E_0 = 18.12 \exp\{1.10 [C/(S + A) - kF]\}$ $k = 8.00$	84.0	7

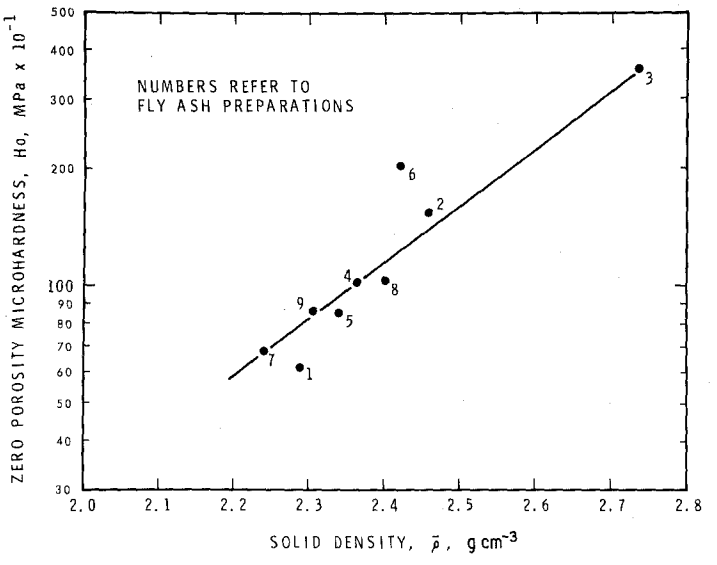

Figure 5 Zero-porosity microhardness versus solid density of autoclaved cement–fly ash mixtures.

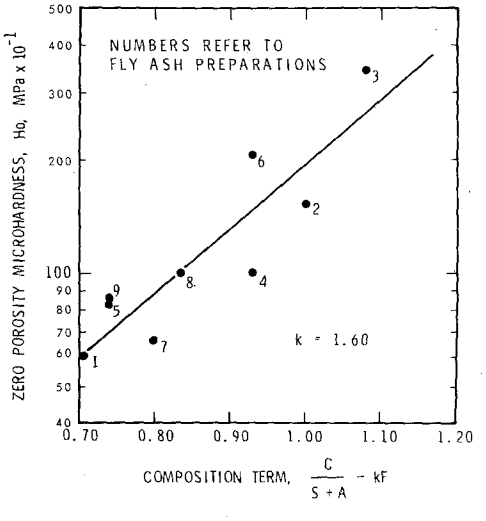

Figure 6 Zero-porosity microhardness versus composition term, $C/(S + A) - kF$.

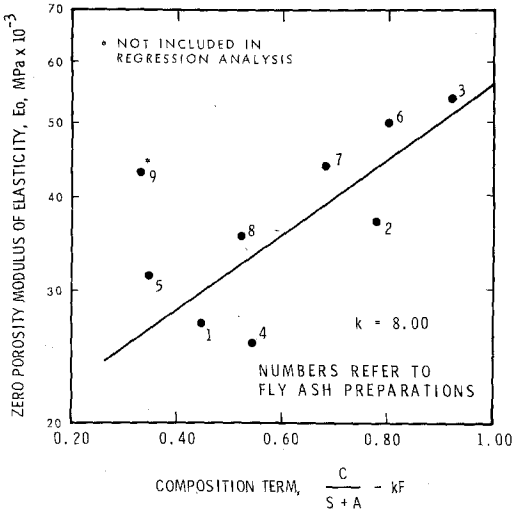

Figure 7 Zero-porosity modulus of elasticity versus composition term, $C/(S + A) - kF$.

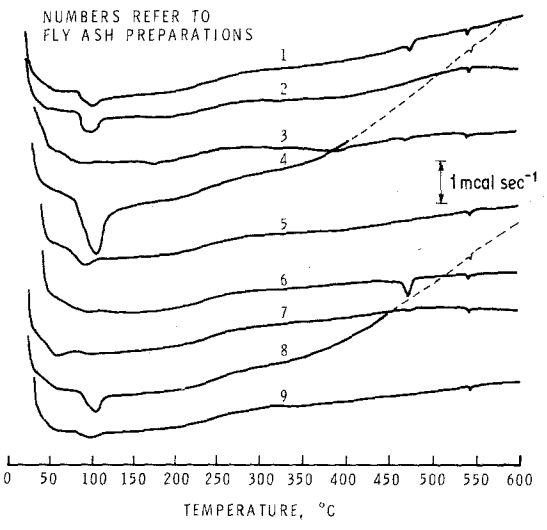

Figure 8 DSC traces of autoclaved cement–fly ash mixtures.

material. These fibres are generally flat, elongated plates having Ca/Si ratios of 0.8 to 1.00, as determined by energy dispersive XRD. Preparation 3 has predominantly the morphology presented in the micrograph and a significant number of sites have Ca/Si ratios of 1.4 to 2.2, suggesting that high lime products such as αC_2SH are present. The remaining preparations have surface textures that appear to be largely amorphous. The smooth areas in preparations 6 and 7 represent C–S–H material – not $Ca(OH)_2$ – with Ca/Si ratios up to 2.0.

3.1.2.3. XRD. X-ray diffraction densitometer traces are plotted in Fig. 10, where tobermorite may easily be detected from the lines of this phase – 11.33, 3.09, 2.94 Å and others. Relatively intense diffractions attributed by Sauman [5] to the hydrogarnet component and not overlapped by lines of the remaining components 5.37, 5.01,

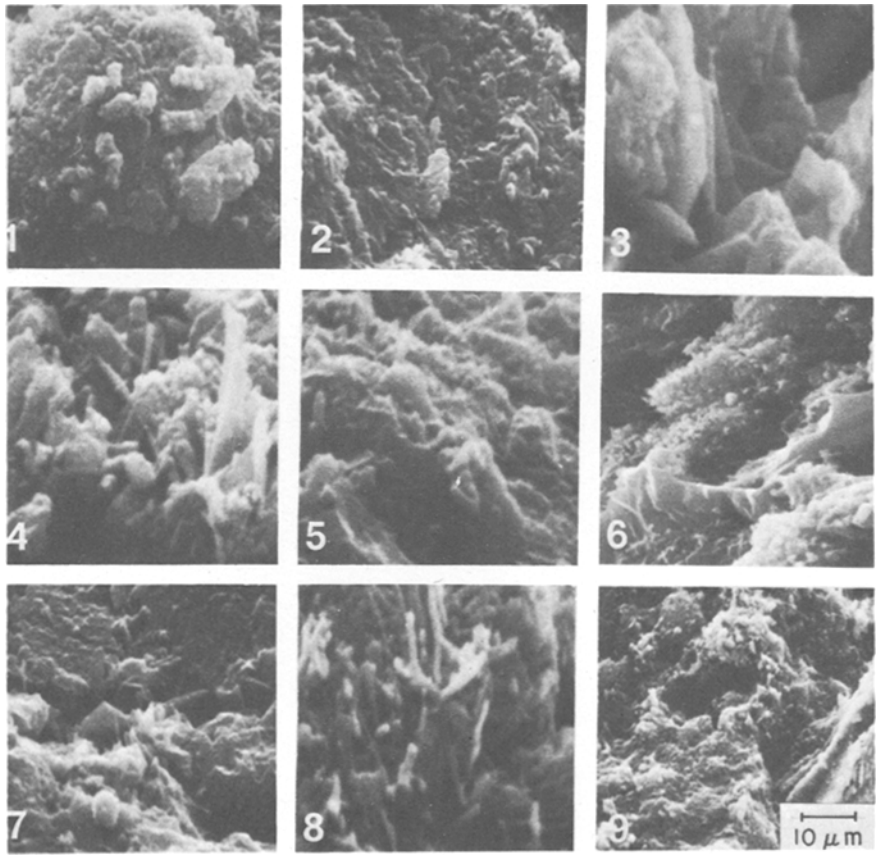

Figure 9 SEM micrographs of autoclaved cement–fly ash mixtures.

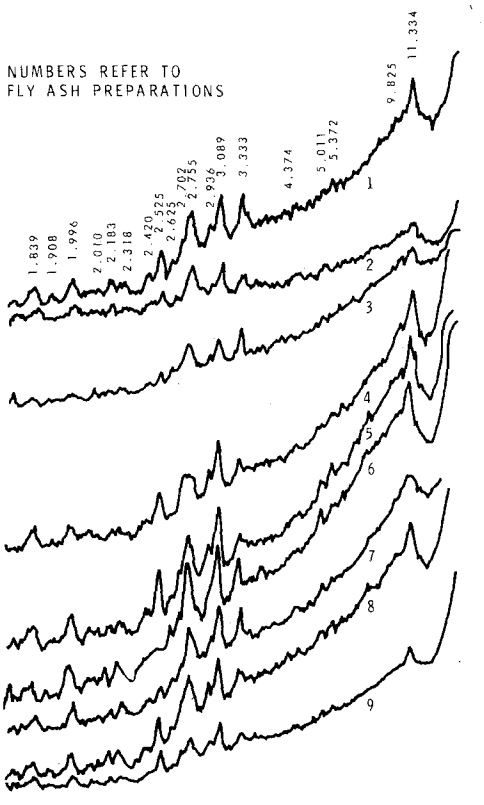

Figure 10 XRD densitometer traces of autoclaved cement–fly ash mixtures.

4.37, 2.75, 2.52, 2.18, 2.00 Å are also visible. Unreacted quartz is present in all samples. No significant quantities of still uncombined $Ca(OH)_2$ were detected. Xonotlite may be present, as the lines at 3.09 and 2.00 Å are strong in preparations 2 and 3, although the 11.3 Å line for tobermorite has a significantly reduced intensity. Preparations 2 and 3 have the highest densities, 2.46 and 2.76 g cm^{-3}; this is indicative of high-density xonotlite. αC_2S hydrate – lines at 2.42, 2.62 and others – contributes significantly to high-density values. Remaining lines for αC_2S hydrate overlap with lines for other phases.

Sauman [5] has argued that the hydrogarnet phase in autoclaved cement–fly ash mixtures probably has the general composition $C_3A_{1-n}F_nS_xH_{6-2x}$ due to Fe-ions in the fly ash glass.

3.2. Practical evaluation: effect of water–solids ratio and composition on mechanical properties

Modulus of elasticity and microhardness data are plotted against C/(S + A) in Figs. 11 and 12. In each there is a family of curves, each curve representing a different water–solid ratio, the lowest water–solid ratio curve having highest values of modulus of elasticity or microhardness. Each curve has at least two maxima and two minima. It is noteworthy that plot points (Fig. 11) for fly ashes 4, 5, 8 and 9 correspond to minimum positions and have maximum Fe_2O_3 contents. In Fig. 12 (microhardness), plot points having maximum positions are for fly ashes 5 and 6. Fly ash 5 has highest Fe_2O_3 content, and fly ash 6 a very low one. It is apparent that Fe_2O_3 content has a direct effect on modulus of elasticity values. The effect on microhardness will be discussed later.

Linear correlations were obtained between modulus of elasticity and a composition term

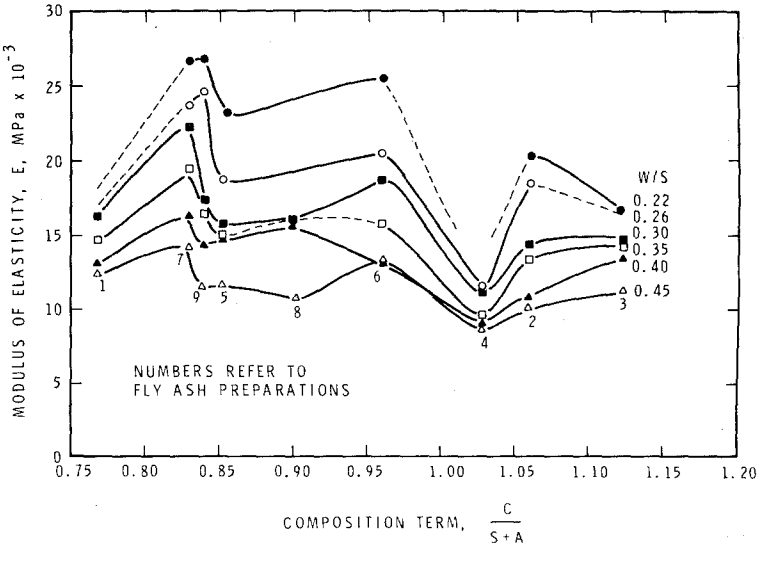

Figure 11 Modulus of elasticity versus composition term C/(S + A) for autoclaved cement–fly ash mixtures.

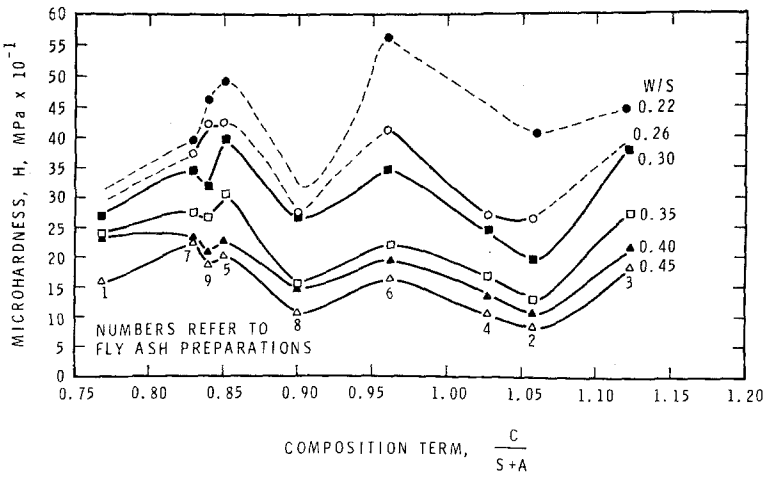

Figure 12 Microhardness versus composition terms C/(S + A) for autoclaved cement–fly ash mixtures.

$[2 - C/(S + A) - kF]$; the regression lines are plotted in Fig. 13 for each water–solid ratio. The significance of the composition term will be discussed at length later. Equations obtained from linear regression analysis are tabulated in Table V. The value of $k = 4.80$ is the value that gives the best correlation for the data analysed.

Microhardness is plotted against $[2 - C/(S + A)]$ in Fig. 14. The addition of $\pm kF$ to the composition term did not significantly affect the nature of the relation. There is a separate curve for each water–solid ratio, with microhardness values for the lowest w/s ratio being the highest. The curves exhibit a minimum at $[2 - C/(S + A)] \simeq 0.93$; then microhardness increases to a maximum for $2 - C/(S + A)$ between 1.04 and 1.10. The minimum is associated with fly ash 2, which has medium Fe_2O_3 content. The maximum is associated with fly ash 6 for w/s = 0.22 and with fly ash 5 for the other w/s ratios. Fly ash 6 has low Fe_2O_3 content and fly ash 5 has high Fe_2O_3 content. These observations will be discussed later.

TABLE V Regression analysis of modulus of elasticity versus composition term

w/s	Regression equation	Correl. coeff., r (%)
0.22	$E = -1.19 + 27.72X^*$	79.6
0.26	$E = -4.40 + 27.81X^*$	79.1
0.30	$E = -1.76 + 20.58X^*$	86.1
0.35	$E = 0.26 + 16.59X^*$	81.2
0.40	$E = 3.00 + 11.83X^*$	66.2
0.45	$E = 1.52 + 11.51X^*$	88.9

$X^* = [2 - C/(S + A) - kF]; k = 4.80$

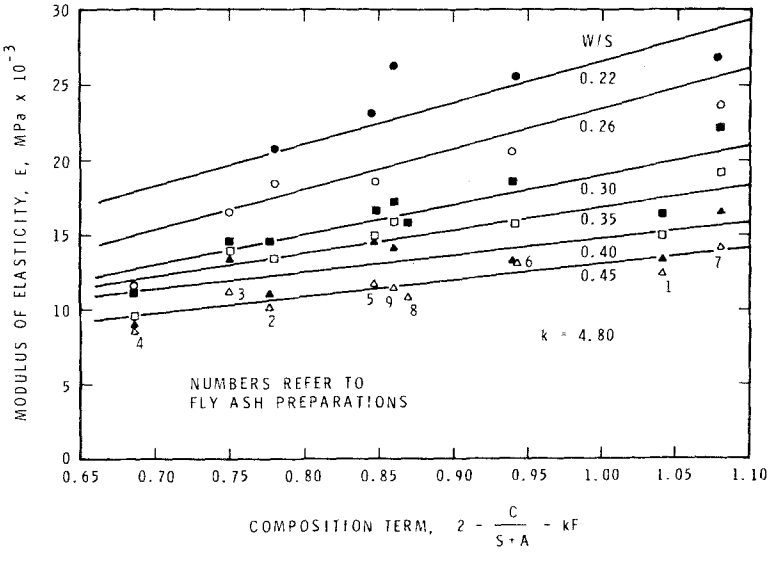

Figure 13 Modulus of elasticity versus composition term, $2 - C/(S + A) - kF$, for autoclaved cement–fly ash mixtures.

3.3. Impregnated systems

3.3.1. Sulphur impregnation

It has been shown that a mixing rule can be used to determine the modulus of elasticity of a sulphur-impregnated porous body and that the impregnated body behaves like a homogeneous two-phase composite [6]. The equation for the composite, derived from Reuss's model is

$$E_c = \left(\frac{V_1}{E_{01}} + \frac{V_2}{E_{02}}\right)^{-1}, \quad (1)$$

where E_c is the modulus of the composite, V_1 and V_2 the volume fraction of the matrix and impregnant, respectively, and E_{01} and E_{02} the moduli of the bulk non-porous matrix material and impregnant, respectively. Values for E_{01} (Table II), obtained by extrapolation of the log modulus of elasticity versus porosity relations, were used to calculate E_c from Equation 1. E_{02} for sulphur is 13.9×10^3 MPa [11]. The values of E_c calculated from Equation 1 compare favourably with the measured values of E_c and the results are recorded in Table VI. The ratio of modulus of elasticity of the composite to modulus of elasticity of the unimpregnated porous body E_c/E_u (Table VI) is 1.15 for fly ash 1 preparations and increases to 2.51 for the fly ash 4 preparation. Increases in microhardness ratio H_c/H_u are also tabulated in Table VI and range from 1.49 to 3.92, with one value as high as 5.51.

TABLE VI Modulus of elasticity and microhardness measurements for sulphur-impregnated fly ash preparations

Fly ash	E_c (MPa × 10^{-3})		E_c/E_u	H_c/H_u
	Eqn. 1	Measured		
1	23.82	22.25	1.15	3.09
2	26.78	30.27	2.11	3.92
3	33.85	30.50	1.83	1.49
4	21.05	23.68	2.51	3.11
5	24.78	24.39	1.64	2.53
6	30.79	24.60	1.56	2.42
7	30.39	24.58	2.15	3.01
8	26.22	24.94	1.70	5.51
9	29.06	27.22	1.57	3.39

4. Discussion

Mechanical property–porosity relations obtained for each fly ash indicate that there is no unique relation for autoclaved cement–fly ash mixtures. Correlations were obtained for zero-porosity modulus of elasticity, E_0, or microhardness, H_0, of the non-porous matrix and density or a composition term, $C/(S + A) - kF$. To understand the significance of the composition term it will be necessary to comment briefly on the general state of existing knowledge of the lime–silica reaction under autoclaved conditions.

On the basis of SEM, DSC and XRD evidence it appears that the fly ash has nearly all reacted. There was only a small amount of $Ca(OH)_2$ detected and no residual fly ash particles were observed. It is assumed, therefore, that under the present autoclave test conditions the reactivity of the fly ash at room temperature is not of major importance.

Helium diffusion experiments showed that helium intake decreased as the density of the hydrated product increased, indicating that less helium was able to enter the structure. Zero-porosity modulus of elasticity and microhardness increase as density of the hydrated product increases, probably due in part to the change in structure indicated by the helium measurements.

In the second section, mechanical properties of the porous bodies were correlated with a composition term, $[2 - C/(S + A) - kF]$. This too, will be elaborated on subsequently, for it is necessary to comment first on lime–silica reactions under autoclave conditions.

In the third section, data demonstrating the potential use of autoclaved cement–fly ash mixtures for sulphur-impregnated systems was presented. This too will be discussed further.

4.1. Lime–silica reaction

The initial reaction on the silica surface yields a lime-rich, poorly crystallized mineral similar to C–S–H(II). When the overall Ca/Si ratio is low (below 1.0), this reaction proceeds until all the lime is used. The following sequence of reactions will eventually take place, C–S–H(II) → C–S–H (I) → tobermorite → xonotlite. When the overall Ca/Si ratio is greater than 1.0, the C–S–H(II) crystallizes to other lime-rich silicates, the most common being αC_2S hydrate.

4.2. Composition terms

Much work has revealed that at normal water–cement ratios, bodies formed with large quantities of αC_2S hydrate ($C/S = 2$) have relatively high porosities; the αC_2S hydrate bonds poorly and these bodies have low strength. Considering this,

a term to correlate with strength of porous bodies would be $2 - C/S$. The capacity of the alumina to combine with some CaO and thus effectively reduce the available CaO for reaction with SiO_2 led to consideration of the parameter $2 - C/(S + A)$. It is recognized that alumina may enter the lattice of the tobermorite type compounds and affect their properties, and together with other impurities, even affect crystallinity. In this work the quantities, C, S, A, F were taken as the total composition of the cement plus fly ash. Thus if there is any proportion of any constituent not available for reaction this approximation will be in error. The observation that the minima for modulus of elasticity versus $C/(S + A)$ corresponded to fly ashes having maximum Fe_2O_3 content, and that maxima corresponded to fly ashes having minimum Fe_2O_3 contents, suggests that Fe_2O_3 was detrimental to high values of modulus of elasticity and that a better correlation would be obtained with the term $2 - C/(S + A) - kF$. Correlation of modulus of elasticity with this term yields straight lines with greatly improved correlation coefficients, confirming the detrimental nature of the iron.

4.3. E_0, H_0 and composition

Zero-porosity modulus of elasticity, E_0, and microhardness, H_0, of high-density crystalline minerals such as αC_2S hydrate are high, although porous bodies composed mainly of these minerals have very low modulus of elasticity and microhardness values. Elimination of porosity considerably reduces the contribution of interparticle bond to strength of the body. Previous studies of autoclaved cement–silica systems indicated that E_0 and H_0 increased as C/S of the hydrated product increased. In this study, E_0 and H_0 increased as the term $C/(S + A) - kF$ increased. It is apparent that Fe_2O_3 has a detrimental effect on the strength of the solid phase, and that the constant k is significantly larger for the curve correlating E_0 with composition ($k = 8.00$ for E_0 curve and $k = 1.60$ for H_0 curve). It is suggested that the presence of Fe_2O_3 in the polycrystalline solid phase influences the effect that grain boundaries and dislocations have on the mechanical properties of the solid; the influence of Fe_2O_3 is apparently much greater for modulus of elasticity than for microhardness. Fe_2O_3 may not alter or modify significantly the failure processes associated with existing crack tips or flaws and hence not significantly affect microhardness measurement involving failure processes. The measurement, however, of modulus of elasticity, which does not involve a failure process, may receive a contribution due to the compressibility of Fe_2O_3.

4.4. E, H, w/s ratio and composition

Modulus of elasticity and microhardness data were plotted against $[2 - C/(S + A) - kF]$. For modulus of elasticity measurements the value of $k = 4.80$ gave the best linear correlation at each water–solid ratio. The effect of Fe_2O_3 on modulus of elasticity was apparently detrimental. The value of $k = 0.0$ for microhardness results indicated that Fe_2O_3 had little effect on microhardness of the porous bodies. The shape of the microhardness curves (Fig. 14) is probably affected by the relative contributions of zero-porosity microhardness, H_0, of the solid phase and strength of the interparticle bonds. The role that these

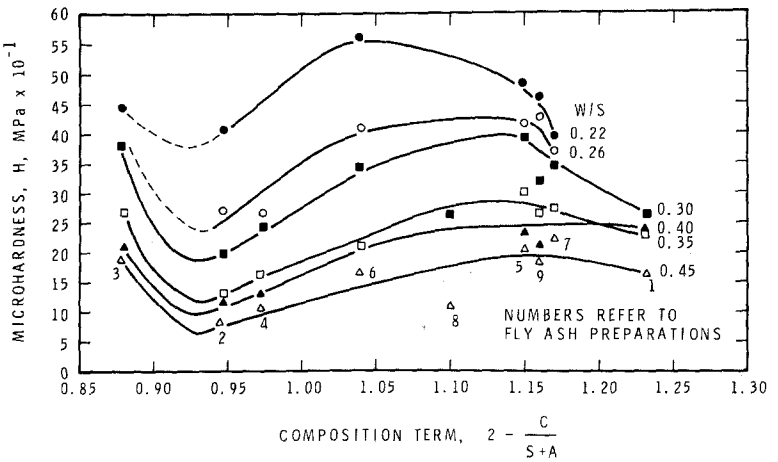

Figure 14 Microhardness versus composition term $2 - C/(S + A)$ for autoclaved cement–fly ash mixtures.

factors play in determining strength of porous bodies is not well understood.

Previous comments on effect of Fe_2O_3 are also applicable.

4.5. Sulphur impregnation

In a previous study, autoclaved cement–silica mixtures with highest values of E_0 and H_0 were superior matrices for sulphur-impregnated system [6]. In the present studies the autoclaved products, when impregnated with sulphur, formed two-phase composites having increased values of modulus of elasticity and microhardness. The Reuss' mixture rule provided reasonable estimates of the elastic moduli of the sulphur-impregnated composites.

Increases in the ratios E_c/E_u and H_c/H_u also depend on E_0 and H_0 as well as on the properties of the unimpregnated porous body, E_u and H_u. The results of this study indicate that, in general, autoclaved cement–fly ash preparations are potentially superior (to room-temperature hydrated cement systems) as binders in sulphur-impregnated cementitious systems in terms of mechanical behaviour. This is principally due to the higher E_0 and H_0 values for these systems. It was observed that factors that affect the magnitude of E_0 and H_0 for autoclaved cement–fly ash mixtures are as follows: C/(S + A) mole ratio, Fe_2O_3 content and density of the hydrated product. Density values depend on phases present in the hydrated product; it has been concluded that an optimum mixture of dense crystalline phases and less dense, poorly crystallized phases exists, giving maximum strength [4, 12]. Fly ash preparation 3, which has the highest C/(S + A) mole ratio, highest product density ($2.76\,g\,cm^{-3}$) and greatest values of E_0 and H_0, appears to have the best potential as a matrix for a sulphur-impregnated building material.

It should be pointed out that for unimpregnated systems, those preparations that have high values of E_0 and H_0 may have low values of E and H at a given porosity. This suggests that when impregnation is not being considered, fly ash 9, for example, would be preferable because equal strengths at lower porosities and probably less permeable concrete are obtained in practice.

Factors affecting the durability of sulphur-impregnated porous bodies have been investigated [13]; all the systems studied were permeable to water and other vapours, whether large increases in mechanical properties were achieved on impregnation or not. Matrices with specific surface areas of approximately $20\,m^2\,g^{-1}$ or less, however, performed well (small expansion with little or no cracking) when exposed to water or other vapours. The specific surface areas of the nine fly ash preparations in this study range from 17.0 to $25.5\,m^2\,g^{-1}$. Their durability on exposure to water is a subject for further study.

5. Conclusions

(1) Modulus of elasticity of porous autoclaved cement-fly ash mixtures, using nine different fly ashes, can be predicted by a relation that depends on w/s ratio and C, S, A and F content and varies directly with the composition term $[2 - C/(S + A) - kF]$.

(2) Microhardness of porous autoclaved cement–fly ash mixtures depends on w/s ratio and the C, S and A content. The F content appears to have little effect on microhardness measurements. A continuous relation exists between microhardness and the composition term $[2 - C/(S + A)]$.

(3) Zero-porosity modulus of elasticity, E_0, and microhardness, H_0, of autoclaved cement–fly ash mixtures depend on C, S, A and F content of the mixture. The logarithms of E_0 and H_0 vary directly with the composition term $C/(S + A) - kF$, which in itself is dependent on the density of the hydrated product. The value of k is much larger for the E_0 relation than for the H_0 relation, indicating that F has a significant effect on E_0 and a minor effect on H_0.

(4) Modulus of elasticity and microhardness of autoclaved cement–fly ash mixtures increase when the mixtures are impregnated with sulphur.

(5) Autoclaved cement–fly ash mixtures having high zero-porisity modulus of elasticity and microhardness have potentially the most suitable matrix for sulphur impregnation.

(6) Chemical analysis of fly ash can serve as a means of providing data enabling the practitioner to predict the strength of autoclaved cement–fly ash mixtures.

Acknowlegements

The authors wish to thank J. J. Wood for his fine work in performing most of the experiments; and G. M. Polomark who carried out the chemical analysis. Thanks are also due to T. G. Clendenning and M. T. Loughborough of Ontario Hydro for providing the fly ash samples and for helpful discussions. This paper is a contribution from the Division of Building Research, National Research

Council of Canada, and is published with the approval of the Director of the Division.

References

1. E. E. BERRY, CANMET Report 76-25 (1976) p. 60.
2. R. C. VALORE, Laboratory evaluation of fly ash and other pozzolans for use in concrete products, Proceedings, Second Ash Utilization Symposium, Pittsburgh (US Department of the Interior, Washington DC, 1970) p. 171.
3. F. MASSAZZA, *Il Cemento* **1** (1976) 3.
4. J. J. BEAUDOIN and R. F. FELDMAN, *Cem. Concr. Res.* **5** (1975) 103.
5. Z. SAUMAN, Study of reactions between CaO or $3CaO \cdot SiO_2$ and β-$2CaO \cdot SiO_2$ and power station fly ashes under hydrothermal conditions, Fifth International Symposium on the Chemistry of Cement, Tokyo, Paper IV-17 (Cement Association of Japan, Tokyo, 1968) p. 122.
6. R. F. FELDMAN and J. J. BEAUDOIN, Structure and properties of porous cement systems and their modification by impregnants, Proceedings, Conference on Hydraulic Cement Pastes: Their Structure and Properties, Sheffield (Cement and Concrete Association, Wexham Springs, Slough, 1976) p. 150.
7. R. F. FELDMAN, *Cem. Concr. Res.* 4 (1973) 1.
8. *Idem, ibid.* **1** (1971) 285.
9. *Idem, Cement Technol.* **3** (1972) 5.
10. P. J. SEREDA, R. F. FELDMAN and E. G. SWENSON, Effect of sorbed water on some mechanical properties of hydrated portland cement pastes and compacts, Highway Research Board, Washington, Special Report 90 (1966) p. 58.
11. J. J. BEAUDOIN and P. J. SEREDA, *Powder Technol.* **13** (1976) 49.
12. J. M. CRENNAN, S. A. S. EL-HEMALY and H. F. W. TAYLOR, *Cem. Concr. Res.* 7 (1977) 493.
13. R. F. FELDMAN and J. J. BEAUDOIN, *ibid.* 8 (1978) 273.

Received 27 October and accepted 20 November 1978.